3D Time Dependent Stokes Vector Radiative Transfer in an Atmosphere-Ocean System Including a Stochastic Interface

George W. Kattawar
Dept. of Physics
Texas A&M University
College Station, TX   77843-4242
phone: (979) 845-1180   fax: (979) 845-2590   email: kattawar@tamu.edu

LONG-TERM GOALS

The major objective of this proposal is to calculate the 3-D, time dependent radiation field both within the ocean and in the atmosphere in the presence of a stochastically varying interface which may also be perturbed by sea foam, air bubbles, surfactants, rain, etc. This study will serve as the genesis to the future evolution of an inversion algorithm whereby one could reconstruct images that have been distorted by the interface between the atmosphere and the ocean or the ocean itself. This study will rely heavily on both the spectral and polarimetric properties of the radiation field to deduce both the sea state and the perturbations produced on it.   A second phase of this study will be to explore the asymptotic polarized light field and to determine how much information can be obtained about the IOP's of the medium by measuring it. The third phase of this proposal will deal with the problem of improving image resolution in the ocean using some novel polarimetric techniques that we are just beginning to explore. Once these studies have been completed using a passive source, it will be rather straightforward to extend them to active sources where we can explore the use of both photo-acoustic and ultrasound-modulated optical tomography to improve image resolution.

OBJECTIVES

The new Navy initiative is focusing on one of the most formidable problems in radiative transfer theory; namely, calculating the full 3D time dependent radiation field (with full Mueller matrix treatment) in a coupled atmosphere-ocean system where the boundary separating the two has both spatial and temporal dependence. Although a great deal of work has been done on obtaining power spectra for ocean waves, I know of no work that has yielded similar results for the radiation field within the ocean. It is clear that as long as the surface has a significant effect on the internal light field, it will leave its signature on the radiation field within the ocean and the relative strength of this field compared to the ambient field will determine the success or failure of inversion algorithms. However, as we go deeper within the ocean we start to enter a region called the asymptotic region where all photons lose memory of their origin and the light field then remains stationary and becomes independent of the azimuthal angle. The depth dependence becomes simply exponential, i.e. $\mathbf{L}(z+h,\theta) = \mathbf{L}(z, \theta) \exp(-kh)$ where k is called the diffusion exponent. It should be noted at this juncture that this asymptotic light field is still polarized which is why we used the bold-faced vector notation. We were the first to compute the degree of polarization for this asymptotic light field for Rayleigh scattering and

1

Report Documentation Page		*Form Approved* *OMB No. 0704-0188*

1. REPORT DATE **30 SEP 2011**	2. REPORT TYPE	3. DATES COVERED **00-00-2011 to 00-00-2011**

4. TITLE AND SUBTITLE
3D Time Dependent Stokes Vector Radiative Transfer in an Atmosphere-Ocean System Including a Stochastic Interface

5a. CONTRACT NUMBER

5b. GRANT NUMBER

5c. PROGRAM ELEMENT NUMBER

6. AUTHOR(S)

5d. PROJECT NUMBER

5e. TASK NUMBER

5f. WORK UNIT NUMBER

7. PERFORMING ORGANIZATION NAME(S) AND ADDRESS(ES)
Texas A&M University,Department of Physics,College Station,TX,77843-3136

8. PERFORMING ORGANIZATION REPORT NUMBER

9. SPONSORING/MONITORING AGENCY NAME(S) AND ADDRESS(ES)

10. SPONSOR/MONITOR'S ACRONYM(S)

11. SPONSOR/MONITOR'S REPORT NUMBER(S)

12. DISTRIBUTION/AVAILABILITY STATEMENT
Approved for public release; distribution unlimited

13. SUPPLEMENTARY NOTES

14. ABSTRACT

15. SUBJECT TERMS

16. SECURITY CLASSIFICATION OF:

a. REPORT **unclassified**	b. ABSTRACT **unclassified**	c. THIS PAGE **unclassified**

17. LIMITATION OF ABSTRACT **Same as Report (SAR)**	18. NUMBER OF PAGES **16**	19a. NAME OF RESPONSIBLE PERSON

Standard Form 298 (Rev. 8-98)
Prescribed by ANSI Std Z39-18

were able to obtain an analytic expression for both the polarized radiation field and the diffusion exponent (see ref. 1). In addition, we were also able to set up a numerical scheme to compute the polarized radiation field as well as the diffusion exponent for any single scattering Mueller matrix. The interesting feature about the asymptotic light field is that it depends profoundly on both the single scattering albedo as well as the phase function of the medium. We also found that substantial errors will occur in both the ordinary radiance and the diffusion exponent if they are calculated from scalar rather than vector theory

APPROACH

 There are several stages to our approach that we will enumerate. The sine qua non for this entire project will be the development of a fully time dependent 3-D code capable of calculating the complete radiation field, i.e. the complete Mueller or Green matrix at any point within the atmosphere-ocean system. This of course implies that both horizontal as well as vertical IOP's must be accounted for. It should also be noted that the code must be capable of handling internal sources as well in order to explore both fluorescence and bioluminescence. At present there are several 3D codes that are able to compute various radiometric quantities in inhomogeneous media; however, as far as we know, none exists which will couple both atmosphere and ocean with a time dependent stochastic interface. One of the earliest 3D radiative transfer (RT) codes was developed by Stenholm, et. al[2] to model thermal emission from spherical and non-spherical dust clouds. It was based on an implicit discretization of the transfer equation in Cartesian frames. To our knowledge, the first 3D-scalar RT code using discrete ordinates was written by Sánchez[3] et al.; however, it did not make use of spherical harmonics and lacked efficiency and accuracy particularly for small viewing angles. The addition of polarization to the 3D discrete ordinates method was done by Haferman[4] et al. Almost concurrently, a 3D-scalar RT code was written by K. F. Evans[5] which used both spherical harmonics and discrete ordinates. This method uses a spherical harmonic angular representation to reduce memory and CPU time in computing the source function and then the RT equation is integrated along discrete ordinates through a spatial grid to model the radiation streams. We have already obtained this code and will use it for validation of our 3D scalar Monte Carlo code for both the atmosphere and ocean components. Several Monte Carlo codes both scalar and vector have been published for solving specialized problems in atmospheric optics usually dealing with finite clouds[6,7,8,9]. Without exception, these codes are using quite primitive, also called "brute force" , methods. None of them will do what we are proposing in our approach to the fully time dependent 3D solution applicable to both atmosphere and ocean. It should be mentioned that we have already successfully added to our Green matrix Monte Carlo code the capability to handle internal sources such as fluorescence, bioluminescence and even thermal emission.

Once we have developed our 3D code to handle both the ocean and atmosphere without the interface included, we will then develop a 3D form of 1D matrix operator theory that we worked out in two seminal papers published in Applied Optics[10,11]. The basic idea of the method is that if one knows the reflection and transmission operators of say two layers, then it is rather straightforward to get the reflection and transmission operators for the combined layer. With this method we can start from an infinitesimal layer and build large and even semi-infinite layers in a rapid way, i.e. if we start with a layer of thickness Δ then in N steps we can reach a thickness of $2^N\Delta$. Another very relevant feature of this method is that it will allow us to add the interface to the "bare" ocean, i.e., one without an interface, to get the combined ocean-interface operator and then add this layer to the atmosphere for the final reflection and transmission operators for the combined system. The question immediately
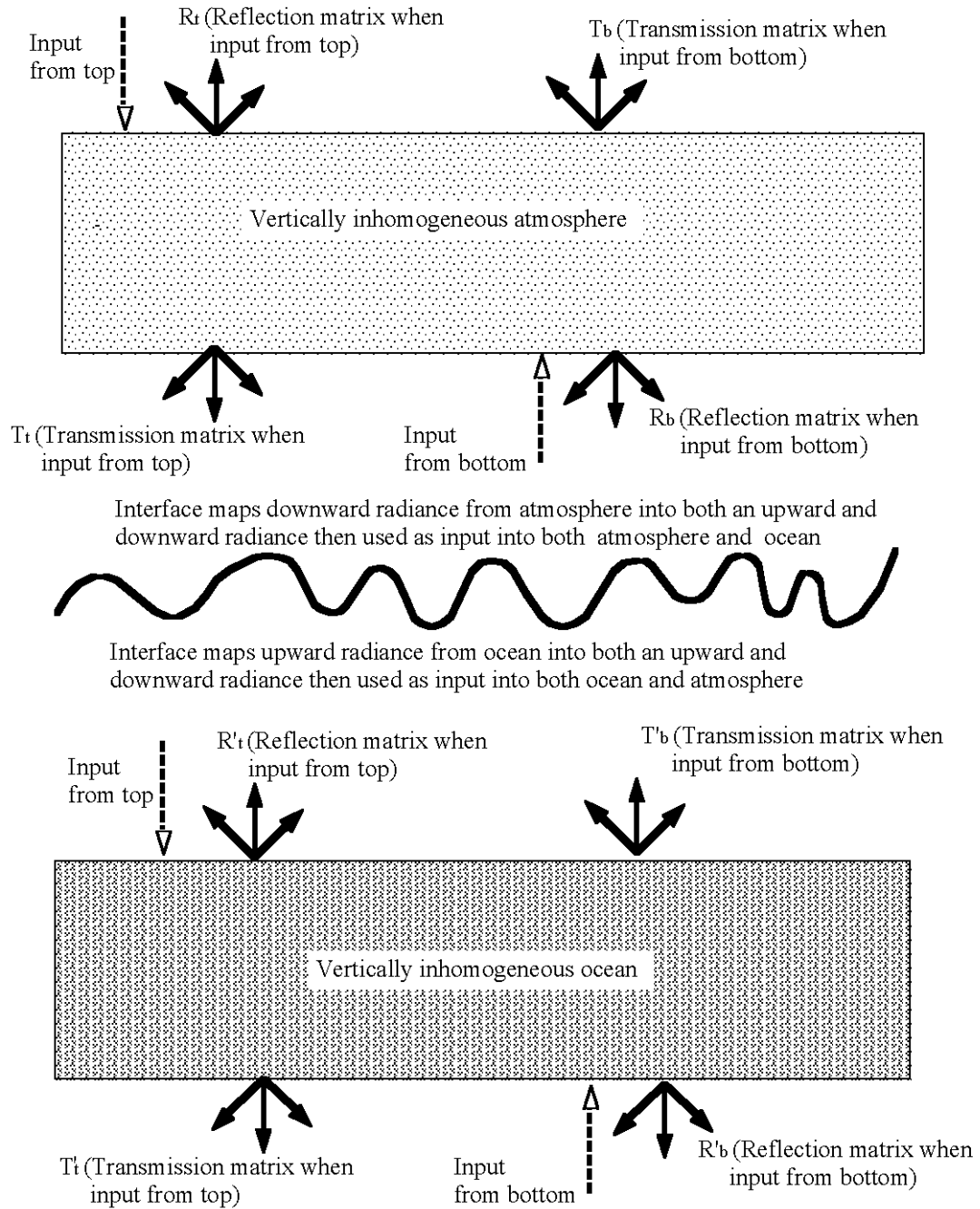
arises is why not solve the entire system at the same time? The answer is that by doing it this way we only have to use the adding feature to combine the time dependent interface thus avoiding performing the entire calculation at each instant in time. This method has also become known as the adding-doubling method. These operators are effectively the impulse response or Green matrix for the upper and lower boundaries of the medium. Therefore, if we know the external radiance input into both upper and lower layers, we can then obtain the output at both the upper and lower boundaries of the combined system. A pictorial description of the method is shown in Fig. 1. It should be emphasized that this method will also handle internal sources as well such as bioluminescence, fluorescence, and even thermal emission. This method can also handle detectors at any interior point in the medium. Another bonus of matrix operator theory is that one can easily obtain the path radiance between source and detector which is a sine qua non for image analysis.

In order to add a interface which is spatially inhomogeneous in the y direction but homogeneous in the x direction, we will need the reflection (R) and transmission (T) operators for both the atmosphere and ocean now as a function of time t and both z and y; namely $R(y-y_0,z,t,\theta,\phi)$ and similarly for T. It is important to note that we only have to obtain the response of the atmosphere or ocean to a single line source at the point y_0 and then using the translational invariance of the medium in the y-direction will have the reflection and transmission operators at every point in the y-direction. The only method we know to create these 2-D operators is Monte Carlo. Once these are obtained, we can use the output from each layer as the input to the surface boundary whose reflection and transmission properties are either known or calculable. For instance if the surface consists of just capillary or gravity waves, then we just need the Fresnel coefficients to give us the requisite reflection and transmission operators for the interface. Now once these operators are obtained then we can use extended matrix operator theory to get the final time dependent radiation field that a detector will see. Let us consider the simplest case where the surface is 1-D and we know its power spectrum. It should be emphasized at this point that it is not sufficient to have just a wave-slope distribution since it will only give us statistically averaged results for the radiance field. The introduction of the spatial and temporal dependent interface destroys the symmetry and makes all 1-D codes essentially useless in this domain.   At each instant in time, the surface will have a distinct shape that will evolve in time. We have developed a method using linear filter theory whereby we can take an ocean power spectrum and using a random number generator crate a realistic surface that will match the original power spectrum and will still exhibit both stationarity and ergodicity.   Now the nice feature about what we are proposing is that we can now concentrate on just the effects of the surface on the detectors since as the surface evolves in time so too will the radiance field as recorded by the detectors. Now both the spatial and temporal profiles will be constantly changing; however, we will have created them from a medium which has been assumed stationary and only the interface produces the time dependence and the horizontal spatial inhomogeneities, i.e. the R and T operators for both the atmosphere and ocean need only to be computed **once.** This is clearly a first-order solution to the more complex problem; however, it should tell us a great deal about future complexities of inversion and also the efficacy of pursuing the next level of difficulty. If the surface is perturbed by foam, bubbles, etc. then these can be added and the matrix operator theory will be used to calculate the effective reflection and transmission operators of the perturbed surface. It should also be stated that this project is enormously computationally intensive; however, the type of codes we will produce are ideally suited for large-scale parallel processors, which we do have access to.

The next level of difficulty is where we will use Monte Carlo methods to compute a full 3-D distribution of the time dependent radiation field, which now may include 3-D inhomogeneities in both

the ocean and atmosphere. This will be a computational tour de force requiring a major new computer program that must be capable of placing IOP's of both the atmosphere and ocean at each point in a large 3-D grid. Matrix operator theory will again be used but it will now be much more complicated since our reflection and transmission operators now become functions of three spatial variables. In fact, the complete solution to this problem could approach the complexity of the general circulation models used in weather forecasting. Due to the large volume of data that will be generated, we will clearly have to develop methods to easily display animated sequences of this time dependence.

There projects were worked on by Dr. Pengwang Zhai, who left for NASA Langley Research Center in August of 2008, and are now being worked on by Dr. Yu You, a postdoctoral research associate.

Rt (Reflection matrix when
input from top)

Input
from top

Tb (Transmission matrix when
input from bottom)

Vertically inhomogeneous atmosphere

Tt (Transmission matrix when
input from top)

Input
from bottom

Rb (Reflection matrix when
input from bottom)

Interface maps downward radiance from atmosphere into both an upward and
downward radiance then used as input into both atmosphere and ocean

Interface maps upward radiance from ocean into both an upward and
downward radiance then used as input into both ocean and atmosphere

R't (Reflection matrix when
input from top)

Input
from top

T'b (Transmission matrix when
input from bottom)

Vertically inhomogeneous ocean

T't (Transmission matrix when
input from top)

Input
from bottom

R'b (Reflection matrix when
input from bottom)

*Fig. 1. Schematic representation on the use of matrix operator theory to calculate the time
dependent radiation field within the ocean*

WORK COMPLETED

a) We have applied the hybrid matrix operator—Monte Carlo (HMOMC) method to simulations
of underwater polarized light field under a dynamic ocean surface. Field data of wave slope
field and water inherent optical properties measured during the RaDyO Santa Barbara Channel

(SBC) experiment have been used as input to the HMOMC calculations. Simulated degree and plane of polarization patterns are found to be qualitatively comparable to measurements of unpolarized and polarized in-water light field also made in the SBC experiment. Analysis of the computer time for the simulation runs reveals that the hybrid model is highly efficient for calculations of multiple frames of polarized light field under a dynamic ocean surface. A paper on this work has been accepted for publication in Journal of Geophysical Research, RaDyO special issue (2011).

b) We have studied the optical volume scattering function (VSF) in a surf zone and the inversion of the VSF for derivation of sediment and bubble particle subpopulations. An irregular hexahedron model has been used for the calculations of VSFs for oceanic particles. A paper on this work has been submitted to Journal of Geophysical Research, RaDyO special issue (2011).

c) We have investigated the effect of ice particle aggregation on light scattering by ice crystals in regions of deep tropical convection. We developed an aggregate representation with 10 ensemble members, each consisting of 4 to 12 hexagonal plates. The averaged scattering properties of aggregate representations computed from either the discrete dipole approximation or improved geometric optics method agree closely with those from 1000 different aggregate geometries. This implies that the aggregation representation provides an accurate and efficient way to represent all aggregates within ice clouds. A paper on this work has been published in Applied Optics, 50, pp. 1065-1081 (2011).

d) We have developed a new physical-geometric optics hybrid (PGOH) method to compute the scattering and absorption properties of ice particles. This method includes analytical considerations of edge effects and amplitude and phase variations over the geometrical wavefront. Therefore, it is good for particles with size parameters as small as ~20. A paper on this work has been published in J. Quant. Spectrosc. Radiat. Transfer, 112, 1492-1508 (2011).

e) We have compared three approximate methods, the surface-integral method, the volume-integral method, and the diffraction plus reflection pattern from ray optics method, that compute scattering of light by dielectric faceted particles. A paper on this work has been published in J. Quant. Spectrosc. Radiat. Transfer, 112, 163-173 (2011).

f) We have made some of the first comprehensive comparisons between simulated and measured underwater polarized light field, including both degree and plane of polarization, in clear oceanic waters. Satisfactory consistencies are observed in the comparisons. Based on model simulation results, we have also shown the limitations of the in-water single scattering approximation in predicting the overall underwater patterns of degree and plane of polarization. A paper on this work has been published in Applied Optics, 50, 4873-4893 (2011).

g) We have made radiative transfer model simulations as a confirmation of the locations of underwater neutral points. Simulation results suggested that the underwater neutral points may move out of the principal plane at longer wavelength in the visible when the diffuse skylight is strong enough. This prediction is consistent with field measurements. A paper on this work has been published on Optics Express, 19, 5942-5952 (2011).

h) We have studied the effects of the polarization state of an incident quasi-monochromatic parallel beam of radiation and the orientation of a hexagonal ice particle with respect to the

incident direction on the extinction process. It is found that the attenuation of a quasi-monochromatic radiation beam by an ice cloud depends on the polarization state of the beam if the ice crystals are not randomly oriented. A paper on this work has been published in J. Quant. Spectrosc. Radiat. Transfer, 112, 2035-2039 (2011).

RESULTS

a) We have used high resolution wave slope measurements and water inherent optical properties (IOPs) measurements as input to our hybrid radiative transfer model, in an effort to reconstruct the highly dynamic polarized radiance field in shallow waters. Figure 2 shows snapshots of wave elevation fields reconstructed from measured wave slope components using a Fourier Transform approach (wave slopes from Chris Zappa, reconstruction algorithm from Howard Schultz). The wave slope measurements were made in the Santa Barbara Channel experiment, with a spatial resolution of roughly 1.3 mm × 1.7 mm and a frame rate of 60 Hz. However, these high resolution measurements cover only a 1 m × 1 m surface patch, which is not adequate for purposes of radiative transfer modeling. We had to extend this surface patch to a 3 m × 3 m one using periodic boundary conditions, such that a detector depth of 1 meter is possible (i.e., the footprint of the Snell cone – the region that the sky radiance can reach – viewed at that depth is within the computational domain).
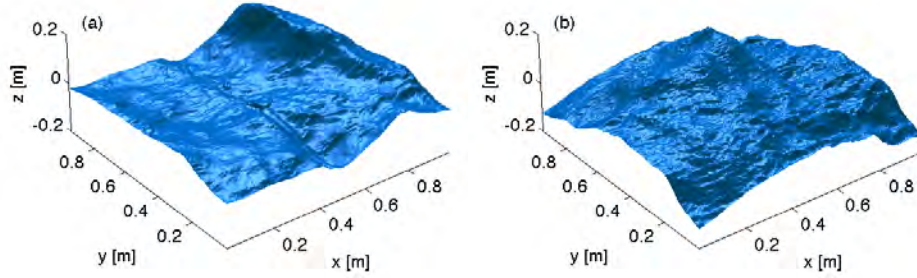
Fig. 2. Snapshots of a dynamic wave elevation field reconstructed from wave slope component measurements in the Santa Barbara Channel: (a) wind speed 5.1 m/s, (b) wind speed 9.3 m/s. The spatial resolution is roughly 1.3 mm × 1.7 mm, and the frame rate is 60 Hz. Shown here are 1 m × 1 m wave patches. They are extended to 3 m × 3 m and used as input to the hybrid radiative transfer model.

Furthermore, we have obtained relevant ocean IOPs from RaDyO collaborators. Field data used in the model simulation include ocean particulate extinction (c_w), single scattering albedo (ω_p) and backscatter factor (b_{back}). The aerosol optical thickness (AOT) is also used. A summary of properties in the simulated atmosphere–surface–ocean system can be found in Table 1.

Table 1. Summary of properties in the simulated ASO system. Entries with an asteroid use field data from RaDyO Santa Barbara Channel experiment. A wavelength of 532 nm was assumed.

| Light source	Solar irradiance	Top-of-atmosphere solar radiation spectrum
Atmosphere	Molecular scattering	Rayleigh phase matrix
	Optical thickness	0.112
	Single scattering albedo	1
	Aerosol scattering	Oceanic aerosols
	Optical thickness*	0.15
Air-sea interface	Wave slopes*	Field data under wind speed 5.1 m/s (extended to 3 m × 3 m)
Ocean	Molecular scattering	Rayleigh phase matrix with depolarization ratio 0.047
	Extinction and albedo	$c_w = 0.046$ m^{-1}, $\omega_w = 0.0457$
	Hydrosol scattering*	Fournier–Forand phase function, where b_{back} is from field data, combined with reduced Rayleigh phase matrix with depolarization ratio 0.1
	Extinction and albedo*	$c_p = 0.6522$ m^{-1}, $\omega_p = 0.9314$
	Physical depth	10 m
Bottom	Lambertian surface	Surface albedo A = 0

To resolve the fine angular distributions when real wave slopes are present, we further improved the hybrid model by treating the direct light part (sun light getting into the ocean without atmospheric scattering, and then multiply-scattered in the ocean) separately. A rather fine angular resolution (1° × 2° in the results shown below) can be achieved in this part. The low-resolution diffuse part (sun light multiple-scattering in the atmosphere and enters the ocean) is then interpolated and added to the direct part. The total radiance field will have the same angular resolution as the direct part, which is necessary to resolve the fine structures in the angular distribution of dynamic radiance fields.

In the simulations, a virtual detector was put at two depths, 0.2 meters and 1 meter. Figure 3 shows the simulated angular distribution of downwelling radiance field viewed at 0.2 meters (left) and 1 meter (center) below the low-sea surface and at 1 meter below the high-sea surface (right). As expected, the structures in the angular distribution due to the wavy surface are even finer when the detector moves further away from the surface and when the surface wind speed increases. One thing to notice here is that the radiance pattern outside of the Snell's cone shows almost no structure due to extremely low signal.
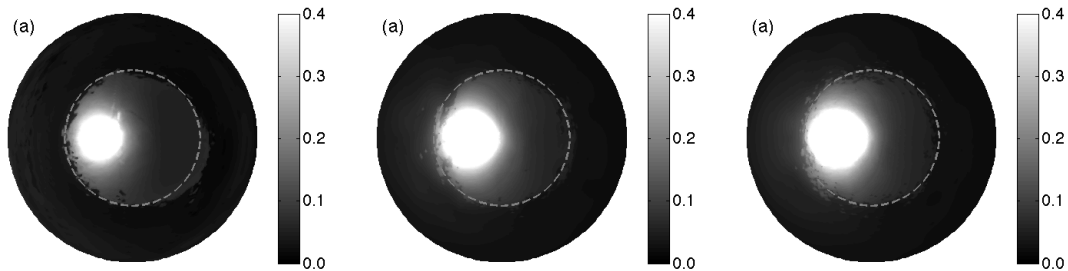

Fig. 3. Simulated underwater downwelling angular distribution of radiance: Left, at 0.2 meters below the low-sea surface; center, at 1 meter below the low-sea surface; and right, at 1 meter below the high-sea surface.

Figure 4 shows the simulated degree of polarization (DoP, left panel) and plane of polarization (PoP, right panel) viewed at 0.2 meters below the low-sea surface. Unlike the radiance pattern, these patterns (especially the PoP pattern) are highly dynamic outside the Snell cone, since the polarization states are largely determined by multiple scattering in the ocean. In the DoP pattern, wave-like structures are found outside of the Snell cone. This implies that the polarization signal contains much more information about the instantaneous wave slope field than the radiance does.
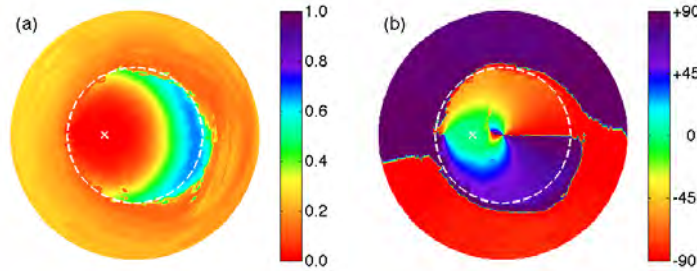

Fig. 4. Simulated downwelling angular distribution of degree of polarization (left) and plane of polarization (right) at 0.2 meters below the low-sea surface.

In Fig. 5 we show comparisons between measured and model simulated underwater angular distributions of radiance, degree of polarization and plane of polarization. The measurements were made by RaDyO researcher Ken Voss in the Santa Barbara Channel experiment, with a solar position at about 55° zenith, a very clear sky, a surface wind speed of about 5 m/s, and a detector depth of 1 meter. In the simulation, we used parameters as close as we could get, and averaged the resultant radiance field over every 0.1 seconds (6 frames) to match up with the integration time associated with the measurements. Although it is unlikely that the instantaneous wave patch is the same (as one can tell from the boundary of the Snell cone), the overall consistencies in all three patterns are surprisingly encouraging. The model simulations failed to reproduce some of the noise in the measured DoP and PoP patterns, which are likely from both instrumentation noise and wave disturbances. This could be partly attributed to the neglect of wave elevations in the model.
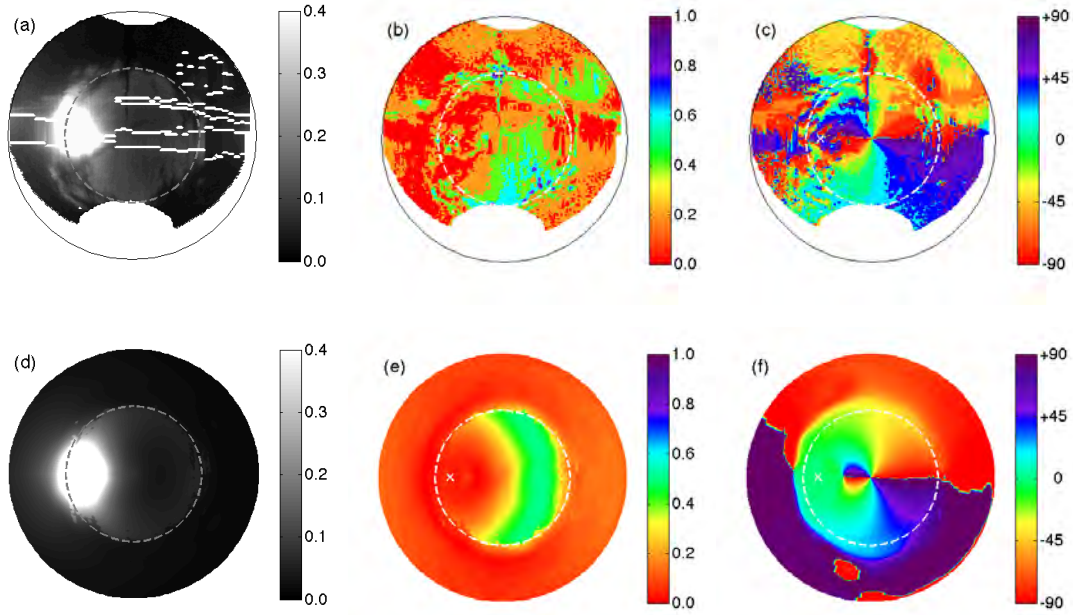
Fig. 5. Comparisons of DPOL-measured (upper panel, from Ken Voss) and model simulated (lower panel) downwelling angular distributions of radiance, degree of polarization, and plane of polarization at 1 meter. Sun is at a zenith angle of about 55°; the sky is clear; and the surface wave speed is about 5 m/s.

Simulated underwater radiances (unpolarized light field) below the high-sea surface were also compared with its counterpart measured by RADCAM. During this measurement, the solar zenith angle was about 45°, the sky was clear, and the surface wind speed was about 11 m/s. The RADCAM instrument operates at the wavelength of 555 (±20) nm. Here we are comparing against the results at 1 m. Figure 6 shows the comparison between the measured (panel (a)) and simulated (panel (b)) underwater downwelling radiance fields in units of W m^{-2} nm^{-1} sr^{-1}. The measured radiance is slightly higher than the simulation (a larger high radiance region, and brighter in the Snell's cone). Despite this discrepancy, the simulation did give dynamic features (such as distortions of the Snell's cone and fine structures at the edge of the Snell's cone) that are qualitatively similar to those seen in the measurement. The measured light field features far more pronounced fine structures and a more distorted Snell's cone. The sources of this discrepancy are two-fold: 1. the instantaneous wave slope field above the measured light field is different from the wave slope measurement used in the model simulation; 2. the model neglected wave elevations.
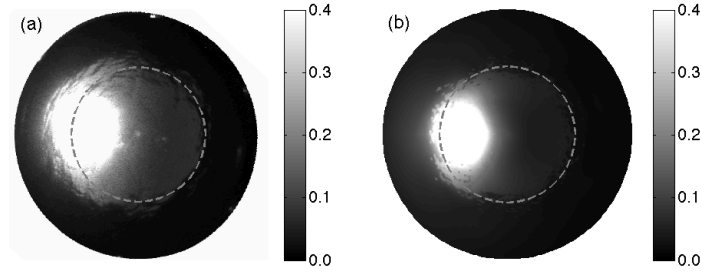
Fig. 6. Comparison of downwelling radiance field at 1 m measured by RADCAM (panel (a)) and simulated by the hybrid model (panel (b)) in units of W m^{-2} nm^{-1} sr^{-1}. The solar zenith angle is 45°, and the surface wind speed is about 10 m/s.

b) In a collaboration with researchers under another MURI project, we compared model simulated underwater light polarization with measurements made by a multispectral polarimeter (CCNY) and by a video polarimeter (UT). In this study we compared not only the degree of polarization but also the plane of polarization, both of which play a critical role for marine animals to use polarization signals for navigation and orientation. Field measurements of water inherent optical properties, particulate scattering volume scattering functions and polarized scattering functions (S12/S11 element) were used in the simulations.

Figures 7 and 8 show the comparisons of the degree of polarization (DoP) angle of polarization (AoP) at nine wavelengths. The model simulations are consistent with the measurements at shorter wavelengths. In the red the measurements are too noisy for a good comparison.

B1; SE = 17.8; VA = 0; z = 1 m
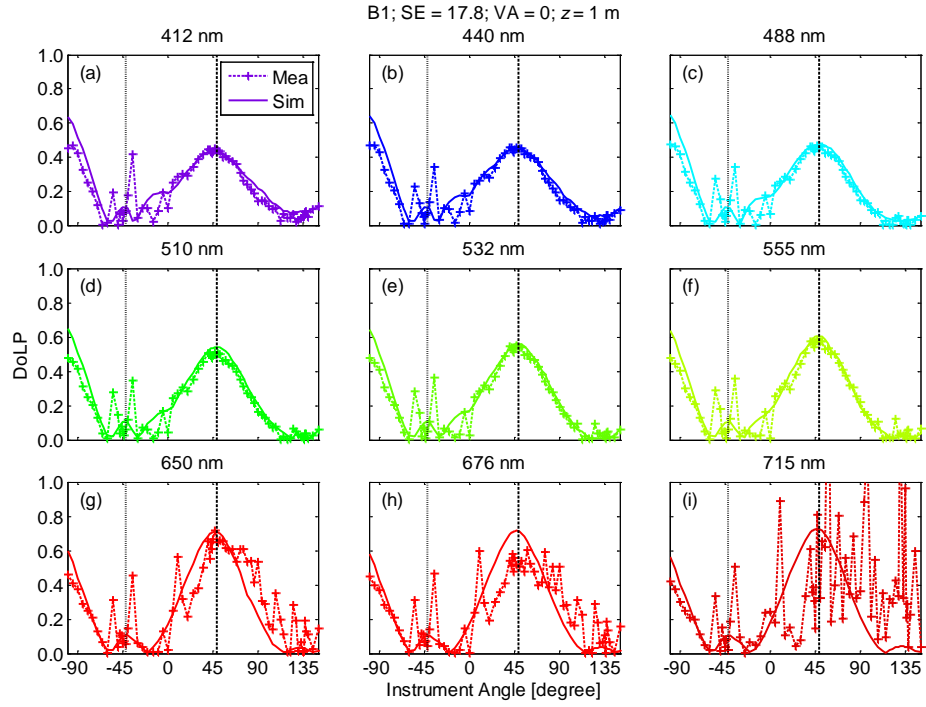
Fig. 7. Degree of polarization (DoP) patterns from CCNY measurements and from simulations at nine wavelengths; the vertical dashed line indicates the angle that corresponds to a 94° scattering angle; the vertical dotted line indicates the edge of the Snell's window, with angles within the window to its left. "SE" stands for "Solar Elevation", "VA" stands for "Viewing Azimuth", and z is the detector depth.


B2; SE = 21.0; VA = 45; z = 1 m
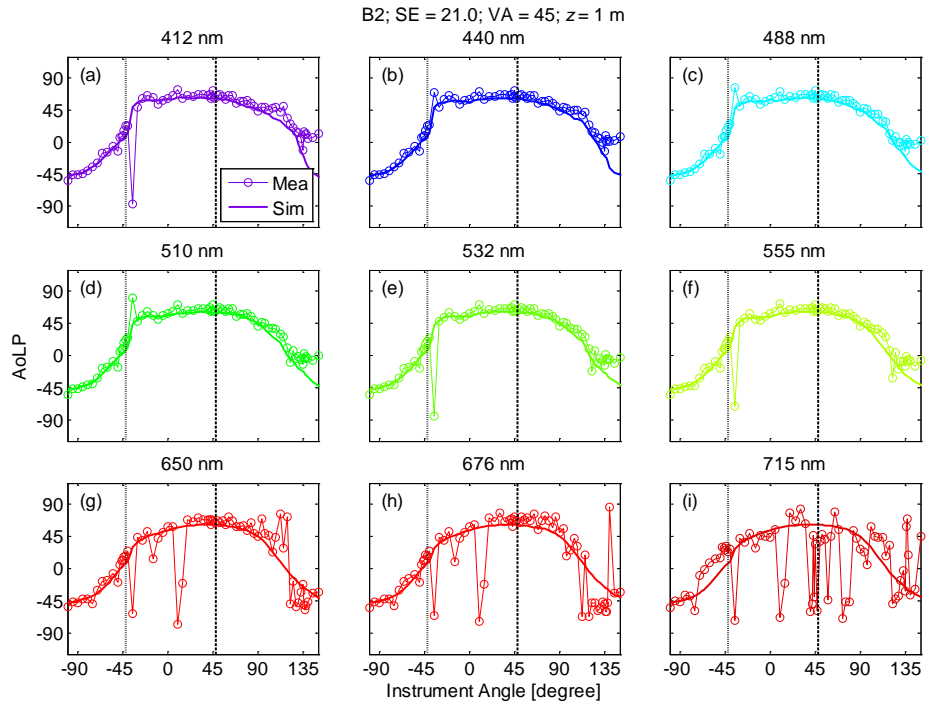
Fig. 8. Same as Fig. 7, but shows patterns of the angle of polarization (AoP).

Figures 9 and 10 shows ta comparison of model simulations against measurements from the UT video polarimeter at the wavelength of 510 nm. The consistency here is not as good since a great deal of estimations were made in determining the viewing angles in the measurement. Nevertheless, the general agreement is encouraging.
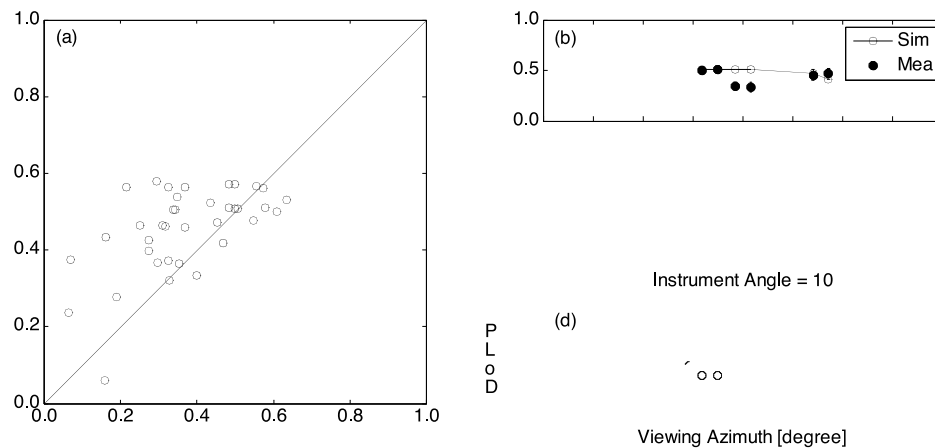
Fig. 9. Comparison of the degree of polarization (DoP) from model simulations and from UT video polarimeter measurements
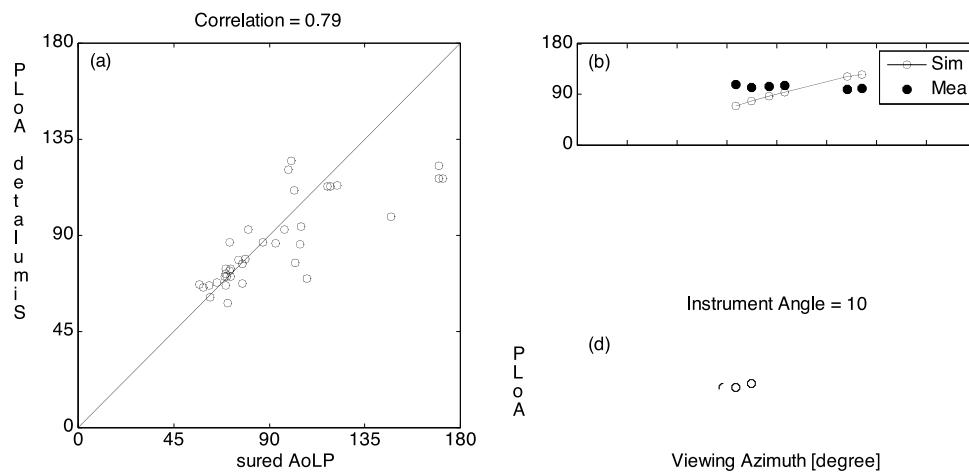
Fig. 10. Same as Fig. 9, but shows the comparison of the angle of polarizatio (AoP).

IMPACT/APPLICATION

The HMOMC code and the fast irradiance code will become powerful tools to investigate the effects of a dynamic wave profile on the radiance field, especially on the polarization states and fast fluctuations of the light field. The fast irradiance code will also be helpful in understanding the fast-varying environment surrounding ocean organisms, which is part of an ONR funded MURI project on underwater camouflage.

TRANSITIONS

Due to the efficiency and versatility of this new code, it will be directly applicable to understanding one of the most formidable problems in global warming, i.e. the effect of broken clouds on the reflectivity of the atmosphere. My colleague, Dr. Ping Yang in the Department of Atmospheric Sciences at TAMU, will use it to interpret the measurements of the satellites, Cloud-Aerosol Lidar and Infrared Pathfinder Satellite Observation (CALIPSO), Moderate Resolution Imaging Spectroradiometer (MODIS), and Polarization and Directionality of the Earth's Reflectances (POLDER). This code can also be used in biomedical studies, such as numerical simulations of the light propagation in skin tissue.

RELATED PROJECTS

We use the results from our other ONR Grant to use as input to our codes in our MURI study of cephalopods.

REFERENCES

1. G. W. Kattawar and G. N. Plass, "Asymptotic Radiance and Po1arization in Optica1ly Thick Media: Ocean and Clouds," Appl. Opt. 5, 3166-3178 (l976).

2. L. G. Stenholm, H. Störzer, and R. Wehrse, "An efficient method for the solution of 3-D Radiative Transfer Problems", JQSRT. 45. 47-56, (1991)

3. A. Sánchez, T.F. Smith, and W. F. Krajewski "A three-dimensional atmospheric radiative transfer model based on the discrete ordinates method", Atmos. Res. 33, 283-308, (1994),

4. J. L. Haferman, T. F. Smith, and W. F. Krajewski, "A Multi-dimensional Discrete Ordinates Method for Polarized Radiative Transfer, Part I: Validation for Randomly Oriented Axisymmetric Particles", JQSRT, 58379-398, (1997)

5. K.F. Evans, "The spherical Harmonics Discrete Ordinates Method for Three-Dimensional Atmospheric Radiative Transfer", J. Atmos. Sci., 55, 429-446, (1998)

6. Q. Liu, C. Simmer, and E. Ruprecht, "Three-dimensional radiative transfer effects of clouds in the microwave spectral range", J, Geophys. Res. 101(D2), 4289-4298, (1996)

7. B. Mayer, "I3RC phase I results from the MYSTIC Monte Carlo model", Extended abstract for the I3RC workshop, Tucson Arizona, 1-6, November 17-19, (1999).

8. L. Roberti and C. Kummerow, "Monte Carlo calculations of polarized icrowave radiation emerging from cloud structires", J, Geophys. Res. 104(D2), 2093-2104, (1999).

9. C. Davis, C. Emde, and R. Harwood, "A 3D Polarized Reversed Monte Carlo Radiative Transfer Model for mm and sub-mm Passive Remote Sensing in Cloudy Atmospheres", Trans. Geophys. and Rem. Sens., Special MicroRad04 Issue, (2004).

10. G. N. P1ass, G. W. Kattawar and F. E. Catchings, "Matrix Operator Theory of Radiative Transfer I. Rayleigh Scattering," Appl. Opt. l2, 314-329 (l973).

11. G. W. Kattawar, G. N. P1ass and F. E. Catchings, "Matrix Operator Theory of Radiative Transfer. II. Scattering from Maritime Haze," Appl. Opt. l2, 1071-1084 (1973).

PUBLICATIONS

1. Y. Xie, P. Yang, G. W. Kattawar, B. A. Baum, and Y. Hu, "Simulation of the optical properties of plate aggregates for application to the remote sensing of cirrus clouds, Appl. Opt., 50, 1065-1081, (2011). [published, refereed].

2. L. Bi, P. Yang, G. W. Kattawar, Y. Hu and B. A. Baum, "Scattering and Absorption of Light by Ice Particles: Solution by a New Physical-Geometric Optics Hybrid Method", Journal of Quant. Spectrosc. Radiat. Transf., 112, 1492-1508, (20110. [published, refereed].

3. L. Bi, P. Yang, G. W. Kattawar, Y. Hu, and B. A. Baum, "Diffraction and External Reflection by Dielectric Faceted Particles", J. Quant. Spectrosc. Radiat. Transfer, 112, (2011). [published, refereed].

4. Y. You, A. Tonizzo, A. A. Gilerson, M. E. Cummings, P. Brady, J. M. Sullivan, M. S. Twardowski, H. M. Dierssen, S. A. Ahmed, and G. W. Kattawar, "Measurements and simulations of polarization states of underwater light in clear oceanic waters", Applied Optics, 50, 4873-48 93, (2011). [published, refereed].

5. K. J. Voss, A. Gleason, H. R. Gordon, G. W. Kattawar, and Y. You, "Discovery of Non-Principal Plane Neutral Points in the In-water Upwelling Polarized Light Field", Optics Express, 19, 5942-5952, (2011). [published, refereed].

6. T. Dickey, G. W. Kattawar, and K. Voss , "Shedding New Light on Light in the Ocean", Physics Today, 44-49,April, (2011). [published, refereed].

7. G. W. Kattawar and Yu You, "Monte Carlo Method", Thermopedia, (2011). [accepted, refereed].

8. G. W. Kattawar and Yu You, "Hybrid Method", Thermopedia, (2011). [accepted, refereed].

9. M. Twardowski, X. Zhang, S. Vagle, J. Sullivan, S. Freeman, H. Czerski, Y. You, L. Bi, and G. W. Kattawar, "The optical volume scattering function in a surf zone inverted to derive sediment and bubble particle subpopulations", Journal of Geophysical Research, RaDyO special issue, (2011). [submitted, refereed].

10. Y. You, G. W. Kattawar, K. J. Voss, P. Bhandari, J. Wei, M. Lewis, C. J. Zappa, and H. Schultz, "Polarized light field under dynamic ocean surfaces: numerical modeling compared with

measurements", Journal of Geophysical Research, RaDyO special issue, (2011). [accepted, refereed].

11. P. Yang, M. Wendisch, L. Bi, G. W. Kattawar, M. Mishchenko, and Y. Hu, "Dependence of extinction cross-section on incident polarization state and particle orientation", J. Quant. Spectrosc. Radiat. Transfer, 112, 2035-2039, (2011). [published, refereed].

12. P. Yang, L. Bi, G. W. Kattawar, R. L. Panetta, "Optical Properties of Nonspherical Atmospheric Particles and Relevant Applications", AAPP Atti della Accademia Peloritani dei Pericolanti, 89, Suppl. No.1, (2011) [published].

13. Y. Xie, P. Yang, G. W. Kattawar, P. Minnis, Y. X. Hu, and D. Wu, Determination of ice cloud models using MODIS and MISR data, Int. J. Remote Sens. [accepted, refereed].

HONORS/AWARDS/PRIZES:

DISTINGUISHED TEXAS SCIENTIST AWARD-2011

Sponsored by the Texas Academy of Science